MATERIALS SCIENCE

Evidence for enormous iodide anion migration in lanthanum oxyiodide–based solid

Nobuhito Imanaka*, Muhammad Radzi Iqbal Bin Misran†, Naoyoshi Nunotani

The I^- ion conduction was demonstrated and quantified in the $La_{0.70}Sr_{0.25}Zn_{0.05}OI_{0.70}$ solid. The I^- ion is considered to be an inferior conductor because of its large ionic size compared to the previously reported conducting ion species. Using modified Tubandt electrolysis, a weight increase at the anodic pellet and a corresponding weight decrease at the cathodic pellet were observed. The weight changes were in good agreement with the theoretical values estimated by considering pure I^- ion migration. Furthermore, the iodine element appeared at the anode, and the iodine concentration at the cathode decreased after electrolysis, indicating that the migrating species was only I^-. This is the first study to elucidate the conduction of iodide ions in solids.

INTRODUCTION

Solid electrolytes are functional materials that have received significant attention owing to their unique property of single ion conduction inside the solid lattice as a charge carrier. In solid electrolytes, it is considered that the ionic conductivity is correlated to the size of the conducting ion species, implying that a small ionic size enables smooth ion conduction. Examples include alkali metal ions, such as the Li^+ ion {0.106 nm, [coordination number (CN) = 8] (*1*)} (*2*–*8*) and Na^+ ion [0.132 nm (CN = 8) (*1*)] (*9*–*13*), and anions, such as the O^{2-} ion [0.126 nm (CN = 6) (*1*)] (*14*–*17*). Li^+ and Na^+ ions are applied in various electrical devices, for example, in all–solid-state and sodium-sulfur batteries (*18*, *19*), owing to their excellent conducting properties. Similarly, O^{2-} ions have already been commercialized as components of oxygen gas sensors, for example, in automotive oxygen gas sensors (*20*). However, conducting anionic species have a relatively small ionic size. Except for the F^- ion, other halide ions are considered weak migrant anions because of their large ionic size.

In the halide series, the bromide anion (Br^-) has the largest ionic size [0.182 nm, (CN = 6) (*1*)] among all the ion species whose conduction was quantified (*21*, *22*). Br^- is also larger than the cesium cation [Cs^+, 0.181 nm (CN = 6) (*1*)], which is the largest cation among all nonradioactive elements. The I^- ion is larger than Br^- and is too large [0.206 nm (CN = 6) (*1*)] to migrate in solids. Such an ion generally acts as a rigid framework maintaining the crystal lattice rather than as the conducting ion species, such as α-AgI of Ag^+ ion-conducting solids (*23*, *24*). Previously, I^- ion conductors have been explored, such as lead iodide (PbI_2) (*25*–*27*), perovskite-type iodides ($CuPbI_3$, $CH_3NH_3PbI_3$, etc.) (*28*–*30*), having low thermal and chemical stability, and iodide-based glasses (PbI_2-PbO, etc.) (*31*–*33*). These have been reported to be a type of I^- ion-conducting solids. However, I^- ion migration in the lattice has not been quantified. It is still unclear whether the I^- ions with a large ionic size can migrate inside the lattice. This study aims to develop a previously unidentified I^- ion conductor whose migrating species is I^- ion and demonstrate macroscopic-only I^- ion migration.

Department of Applied Chemistry, Faculty of Engineering, Osaka University, 2-1 Yamadaoka, Suita, Osaka 565-0871, Japan.
*Corresponding author. Email: imanaka@chem.eng.osaka-u.ac.jp
†Present address: Mitsubishi Materials Corporation, 1002-14 Mukohyama, Naka, Ibaraki 311-0102, Japan.

The critical issue is the precise selection of the crystal structure suitable for iodide ion conduction with high chemical stability. Our work focused on lanthanum oxyiodide (LaOI) with the tetragonal matlockite (PbFCl)–type structure (*P4*/*nmm*) (*34*), which is a layered structure along the *c* axis consisting of a rigid fluorite-type LaO layer and an I^- layer (Fig. 1A). In the LaOI solid, the La^{3+} ion is coordinated to four O^{2-} and four I^- ions. The I^- ions in the distinctive I^- layer are expected to migrate in the *ab* plane. Recently, topotactic anion exchange in LaOI was reported, suggesting the iodide ion diffusion in the lattice (*35*). In addition to its suitable structure for ion conduction, LaOI has significantly high thermal and chemical stabilities than the simple iodide (LaI_3) (*36*). It contains higher-valent O^{2-} ions compared to I^- ions, leading to strong bonding with surrounding La^{3+} cations. For the conduction of I^- ions having large ionic sizes, it is essential to introduce I^- ion vacancies and control the lattice size. We prepared a $La_{0.70}Sr_{0.25}Zn_{0.05}OI_{0.70}$ solid, in which the La^{3+} sites in the LaOI lattice were partially replaced by lower-valent Sr^{2+} and Zn^{2+} to form the I^- ion vacancies and control the lattice size, owing to the larger ionic size of Sr^{2+} [0.140 nm (CN = 8) (*1*)] and smaller ionic size of Zn^{2+} [0.104 nm (CN = 8) (*1*)] than that of La^{3+} [0.130 nm (CN = 8) (*1*)]. In addition, since Zn has high electronegativity [1.65 (*37*)] compared to La [1.1 (*37*)] and Sr [0.95 (*37*)], a strong bonding with the surrounding anions is formed, which is effective to maintain the LaOI lattice even in the case of the large amount of the I^- ion vacancies. For the $La_{0.70}Sr_{0.25}Zn_{0.05}OI_{0.70}$ solid, the macroscopic I^- ion conduction in the LaOI-based solid was demonstrated.

RESULTS AND DISCUSSION

$La_{0.70}Sr_{0.25}Zn_{0.05}OI_{0.70}$ was synthesized by the conventional solid-state reaction method, where the composition was optimized to show the highest conductivity (fig. S1). Figure 1B shows the x-ray powder diffraction (XRD) pattern of $La_{0.70}Sr_{0.25}Zn_{0.05}OI_{0.70}$ along with the data of LaOI. The pattern was identified to be a single-phase matlockite-type structure. The replacement of the La^{3+} sites for Sr^{2+} and Zn^{2+} was confirmed by the change in the lattice volume (fig. S1B), where the lattice volume of $La_{0.70}Sr_{0.25}Zn_{0.05}OI_{0.70}$ (0.1591 nm^3) was larger than that of LaOI (0.1567 nm^3). To investigate the formation of the I^- ion vacancies in $La_{0.70}Sr_{0.25}Zn_{0.05}OI_{0.70}$, x-ray fluorescence (XRF) analysis was performed. The measured composition was estimated to be $La_{0.73}Sr_{0.23}Zn_{0.05}O_{0.99}I_{1-x}$ [x(vacancy) = 0.26], similar

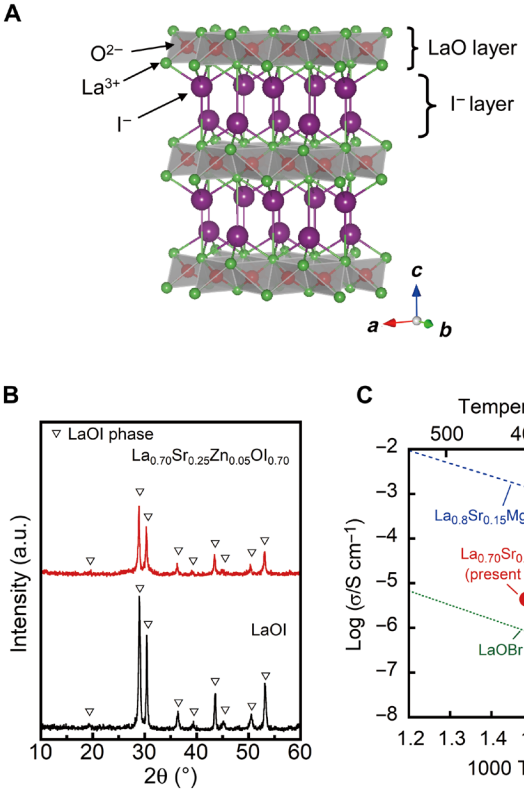

Fig. 1. Crystal structure and conductivity. (**A**) Crystal structure of LaOI (*34*), drawn by VESTA (*39*). (**B**) XRD patterns of $La_{0.70}Sr_{0.25}Zn_{0.05}OI_{0.70}$ and LaOI solids. (**C**) Temperature dependence of the conductivity for the $La_{0.70}Sr_{0.25}Zn_{0.05}OI_{0.70}$ and LaOI solids along with the data of LaOBr-based materials (*22*). a.u., arbitrary units.

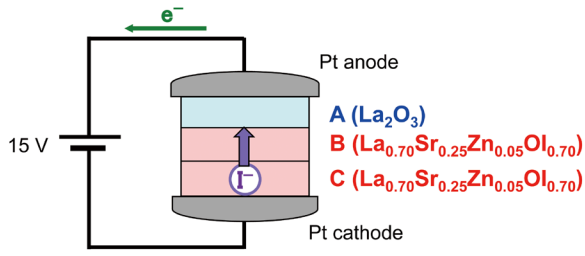

Fig. 2. Schematic illustration of the modified Tubandt electrolysis using one La_2O_3 (pellet A) and two $La_{0.70}Sr_{0.25}Zn_{0.05}OI_{0.70}$ pellets (pellets B and C) sandwiched between two Pt electrodes.

to the feed composition. Therefore, it is confirmed that the introduction of lower-valent Sr^{2+} and Zn^{2+} compared to La^{3+} was compensated by the formation of the I^- and not the O^{2-} vacancies.

Figure 1C shows the temperature dependence of the conductivity of $La_{0.70}Sr_{0.25}Zn_{0.05}OI_{0.70}$ and LaOI. For comparison, the conductivities of the LaOBr-based materials (*22*) were also plotted. The conductivity considerably improved by introducing Sr^{2+} and Zn^{2+}, and the value of 4.4×10^{-6} S cm^{-1} at 400°C was approximately 70 times higher than that of LaOI. This improvement in the conductivity might be due to the increase in I^- ion vacancies, which contribute to the smooth I^- conduction. In addition, the large lattice volume is considered to enhance the conductivity due to the expansion of the large–ionic size I^- conduction pathway. Nevertheless, the conductivity of $La_{0.70}Sr_{0.25}Zn_{0.05}OI_{0.70}$ was lower than that of the Br^- ion-conducting $La_{0.80}Sr_{0.15}Mg_{0.05}OBr_{0.80}$ solid owing to the large ionic size of the I^- ion. LaOI also showed a lower conductivity than LaOBr.

For the $La_{0.70}Sr_{0.25}Zn_{0.05}OI_{0.70}$ solid with high conductivity, the conducting species was investigated and quantified using the modified Tubandt electrolysis (*38*). This electrolysis was performed using one La_2O_3 (pellet A) and two $La_{0.70}Sr_{0.25}Zn_{0.05}OI_{0.70}$ pellets (pellets B and C) sandwiched between two Pt electrodes, as shown in Fig. 2. After applying a DC voltage higher than the decomposition voltage (approximately 0.7 V), the mass changes corresponding to the conducting species can be estimated. In the case of the I^- ion conduction, $La_{0.70}Sr_{0.25}Zn_{0.05}OI_{0.70}$ at the cathode (pellet C) will decompose owing to the generation of the I^- ion, which macroscopically conducts via the middle pellet (B), and I^- reacts with La_2O_3 (pellet A) to form LaOI. The expected chemical reactions are as follows

$$\text{Cathode: } \frac{10}{7}La_{0.70}Sr_{0.25}Zn_{0.05}OI_{0.70} + \frac{1}{4}O_2 + e^- \rightarrow \frac{1}{2}La_2O_3 + \frac{5}{14}SrO + \frac{1}{14}ZnO + I^- \quad (1)$$

$$\text{Anode: } \frac{1}{2}La_2O_3 + I^- \rightarrow LaOI + \frac{1}{4}O_2 + e^- \quad (2)$$

These reactions will lead to the mass increase of pellet A and the mass decrease of pellet C. Considering other species such as O^{2-}, e^-, h^+, proton, and cations (La^{3+}, Sr^{2+}, and Zn^{2+}), if the conducting species is O^{2-}, no mass change should be observed due to the continuous supply of O^{2-} by atmospheric O_2. Similarly, the electron (e^- or h^+) or proton migration would cause no weight change for each pellet. For the cation (La^{3+}, Sr^{2+}, or Zn^{2+}) conduction, $La_{0.70}Sr_{0.25}Zn_{0.05}OI_{0.70}$ decomposes at the middle pellet (pellet B), and the generated cation may be forced to migrate toward the cathodic surface (pellet C), resulting in the reduction of the cation to the metal state followed by immediate oxidation due to atmospheric oxygen gas. As an example, the possible reactions in the case of La^{3+} conduction are described below

$$\text{Middle pellet: } \frac{10}{21}La_{0.70}Sr_{0.25}Zn_{0.05}OI_{0.70} \rightarrow \frac{1}{3}La^{3+} + \frac{5}{42}SrO + \frac{1}{42}ZnO + \frac{1}{6}I_2 + \frac{1}{6}O_2 + e^- \quad (3)$$

$$\text{Cathode: } \frac{1}{3}La^{3+} + e^- \rightarrow \frac{1}{3}La \quad (4)$$

$$\frac{1}{3}La + \frac{1}{4}O_2 \rightarrow \frac{1}{6}La_2O_3 \quad (5)$$

These chemical equations imply that the weight of pellet B would decrease and that of pellet C would increase. The theoretical values (Δm_{cal}) for each of the conducting species can be estimated from the total electric charge (Q) corresponding to the electrolysis. The detailed theory is explained in the Supplementary Materials.

Before and after electrolysis, each pellet was weighed to obtain the mass change (Δm_{obs}). To exclude the change during the electrolysis at the elevated operating temperature, the mass change in each pellet was compensated by using reference pellets of La_2O_3 and $La_{0.70}Sr_{0.25}Zn_{0.05}OI_{0.70}$, which were embedded without electrolysis near the electrolytic cell. The calculation method is described in the

Table 1. Observed and calculated mass changes for two $La_{0.70}Sr_{0.25}Zn_{0.05}OI_{0.70}$ pellets and one La_2O_3 pellet after the modified Tubandt electrolysis performed under two different conditions.

Condition	Q/mC	Sample	Δm_{obs}/mg	Δm_{cal}/mg ($\Delta m_{obs}/\Delta m_{cal}$)				
				I^-	O^{2-}, e^-, or H^+	La^{3+}	Sr^{2+}	Zn^{2+}
400°C, 15 V, 5 days	149.2	A (La_2O_3)	+0.167	+0.184 (91%)	0	0	0	0
		B ($La_{0.70}Sr_{0.25}Zn_{0.05}OI_{0.70}$)	−0.0004	0	0	−0.145 (7%)	−0.338 (3%)	−1.35 (1%)
		C ($La_{0.70}Sr_{0.25}Zn_{0.05}OI_{0.70}$)	−0.174	−0.184 (95%)	0	+0.084 (−208%)	+0.080 (−218%)	+0.06 (−277%)
400°C, 15 V, 7 days	201.4	A (La_2O_3)	+0.220	+0.248 (89%)	0	0	0	0
		B ($La_{0.70}Sr_{0.25}Zn_{0.05}OI_{0.70}$)	+0.048	0	0	−0.196 (−24%)	−0.456 (−10%)	−1.82 (−3%)
		C ($La_{0.70}Sr_{0.25}Zn_{0.05}OI_{0.70}$)	−0.239	−0.248 (96%)	0	+0.113 (−211%)	+0.108 (−221%)	+0.09 (−281%)

Table 2. Measured molar ratios for each pellet after the electrolysis was performed by applying 15 V at 400°C for 5 days.

Sample	I	O	La	Sr	Zn
A (La_2O_3)	0.48%	59.62%	39.90%	0%	0%
B ($La_{0.70}Sr_{0.25}Zn_{0.05}OI_{0.70}$)	26.99%	36.39%	26.56%	8.25%	1.81%
C ($La_{0.70}Sr_{0.25}Zn_{0.05}OI_{0.70}$)	26.41%	36.88%	26.74%	8.17%	1.80%
Ref (La_2O_3)	0%	60.00%	40.00%	0%	0%
Ref ($La_{0.70}Sr_{0.25}Zn_{0.05}OI_{0.70}$)	27.04%	36.36%	26.55%	8.24%	1.81%

Supplementary Materials. The modified electrolysis was performed by applying 15 V at 400°C for 5 or 7 days in atmospheric air, and the obtained results are tabulated in Table 1. The observed mass change at the anode (pellet A) increased, and a corresponding decrease was obtained at the cathode (pellet C) for the two different electrolytic conditions. In addition, no significant mass change was observed in the middle pellet (pellet B). These reproducible mass changes clearly indicate that the conducting species are I^- ions and not O^{2-}, e^-, h^+, La^{3+}, Sr^{2+}, or Zn^{2+}. Furthermore, the observed mass changes were in agreement with the calculated values, where the ratio of the observed mass change to the theoretical value was estimated to be approximately 90%. For the pellet A (La_2O_3) surface in contact with pellet B, the LaOI phase was additionally detected using the XRD measurement (fig. S2), supporting the I^- conduction (Eq. 2).

To obtain further evidence on the I^- conduction, each pellet, after the modified Tubandt electrolysis, was homogeneously pulverized, and the change in the elemental ratio was determined using XRF analysis (Table 2). Although La_2O_3 is composed of La and O, the iodine element was detected in the anodic pellet A [0.48 mole percent (mol %)]. On the other hand, the iodine ratio in cathodic pellet C (26.41 mol %) was appreciably lower than that in middle pellet B (26.99 mol %) and the corresponding reference (27.04 mol %). These results indicate that the source of the mass changes for pellets A and C is the I^- ion migration from pellet C toward pellet A. Therefore, from the mass and elemental changes, the quantitative I^- ion conduction was demonstrated in $La_{0.70}Sr_{0.25}Zn_{0.05}OI_{0.70}$.

In summary, we have successfully identified and quantified I^- ion conduction in $La_{0.70}Sr_{0.25}Zn_{0.05}OI_{0.70}$. However, the I^- ion, owing to its large ionic size, is generally considered to be a constituent component of the lattice and not the conducting ion species. To the best of our knowledge, this is the first report that demonstrates a quantitative pure I^- ion conduction inside the solid lattice.

MATERIALS AND METHODS

Sample preparation

$La_{1-x-y}Sr_xZn_yOI_{1-x-y}$ samples were prepared using the conventional solid-state reaction method. Powders of La_2O_3 (99.99%; Shin-Etsu Chemical), $Sr(NO_3)_2$ (99.9%; Wako Pure Chemical), $Zn(NO_3)_2{\cdot}6H_2O$ (≥99.0%; Kishida Chemical), and NH_4I (99.5%; Kanto Chemical) in a molar ratio of $(1-x-y):2x:2y:4(1-x-y)$ were mixed using an agate mortar and preheated at 400°C for 12 hours under Ar flow (10 ml min^{-1}). The resulting powder was pressed into a pellet by uniaxial pressing at ca. 70 kN with diameter and thickness of 13 and 2 mm, respectively. The pellet was calcined at 400°C for 12 hours under Ar flow (10 ml min^{-1}) several times until a single phase was obtained.

Characterization

The obtained samples were identified using XRD (SmartLab, Rigaku) measurement using Cu Kα radiation (40 kV, 30 mA) in the 2θ range from 10° to 70°. The lattice volume was calculated from the XRD peak angles, refined by using α-Al_2O_3 as an internal standard. XRF (EDX-800, Shimadzu) analysis was performed to confirm the composition. To investigate the electrochemical properties, the sample powder was pelletized by uniaxial pressing at ca. 70 kN with diameter and thickness of 10 and 1 mm, respectively, followed by the sintering at 400°C for 12 hours under Ar flow (10 ml min^{-1}). The obtained pellet was polished with waterproof abrasive papers,

and then, platinum-sputtered layers were formed on the centers of opposite surfaces using an ion coater (IB-3, Eiko). The AC conductivity (σ) of the pellets was measured using the complex impedance method (1260 impedance per gain analyzer, Solartron) in the frequency range between 5 Hz and 13 MHz at temperatures between 400° and 300°C.

SUPPLEMENTARY MATERIALS

Supplementary material for this article is available at https://science.org/doi/10.1126/sciadv.abh0812

REFERENCES AND NOTES

1. R. D. Shannon, Revised effective ionic radii and systematic studies of interatomic distances in halides and chalcogenides. *Acta Crystallogr. Sect. A* **32**, 751–767 (1976).
2. H. Y.-P. Hong, Crystal structure and ionic conductivity of $Li_{14}Zn(GeO_4)_4$ and other new Li^+ superionic conductors. *Mater. Res. Bull.* **13**, 117–124 (1978).
3. G. Adachi, N. Imanaka, H. Aono, Fast Li^+ conducting ceramic electrolytes. *Adv. Mater.* **8**, 127–135 (1996).
4. S. Stramare, V. Thangadurai, W. Weppner, Lithium lanthanum titanates: A review. *Chem. Mater.* **15**, 3974–3990 (2003).
5. R. Murugan, V. Thangadurai, W. Weppner, Fast lithium ion conduction in garnet-type $Li_7La_3Zr_2O_{12}$. *Angew. Chem. Int. Ed.* **46**, 7778–7781 (2007).
6. S. Gao, T. Broux, S. Fujii, C. Tassel, K. Yamamoto, Y. Xiao, I. Oikawa, H. Takamura, H. Ubukata, Y. Watanabe, K. Fujii, M. Yashima, A. Kuwabara, Y. Uchimoto, H. Kageyama, Hydride-based antiperovskites with soft anionic sublattices as fast alkali ionic conductors. *Nat. Commun.* **12**, 201 (2021).
7. N. Flores-González, N. Minafra, G. Dewald, H. Reardon, R. I. Smith, S. Adams, W. G. Zeier, D. H. Gregory, Mechanochemical synthesis and structure of lithium tetrahaloaluminates, $LiAlX_4$ (X = Cl, Br, I): A family of Li-ion conducting ternary halides. *ACS Mater. Lett.* **3**, 652–657 (2021).
8. H. Maekawa, M. Matsuo, H. Takamura, M. Ando, Y. Noda, T. Karahashi, S. Orimo, Halide-stabilized $LiBH_4$, a room-temperature lithium fast-ion conductor. *J. Am. Chem. Soc.* **131**, 894–895 (2009).
9. Y.-F. Y. Yao, J. T. Kummer, Ion exchange properties of and rates of ionic diffusion in beta-alumina. *J. Inorg. Nucl. Chem.* **29**, 2453–2475 (1967).
10. J. B. Goodenough, H. Y.-P. Hong, J. A. Kafalas, Fast Na^+-ion transport in skeleton structures. *Mater. Res. Bull.* **11**, 203–220 (1976).
11. A. Hayashi, K. Noi, A. Sakuda, M. Tatsumisago, Superionic glass-ceramic electrolytes for room-temperature rechargeable sodium batteries. *Nat. Commun.* **3**, 856 (2012).
12. Y. Qie, S. Wang, S. Fu, H. Xie, Q. Sun, P. Jena, Yttrium-sodium halides as promising solid-state electrolytes with high ionic conductivity and stability for Na-ion batteries. *J. Phys. Chem. Lett.* **11**, 3376–3383 (2020).
13. M. Matsuo, S. Kuromoto, T. Sato, H. Oguchi, H. Takamura, S. Orimo, Sodium ionic conduction in complex hydrides with $[BH_4]^-$ and $[NH_2]^-$ anions. *Appl. Phys. Lett.* **100**, 203904 (2012).
14. D. W. Strickler, W. G. Carlson, Ionic conductivity of cubic solid solutions in the system $CaO\text{-}Y_2O_3\text{-}ZrO_2$. *J. Am. Ceram. Soc.* **47**, 122–127 (1964).
15. J. B. Goodenough, J. E. Ruiz-Diaz, Y. S. Zhen, Oxide-ion conduction in $Ba_2In_2O_5$ and $Ba_3In_2MO_8$ (M = Ce, Hf, or Zr). *Solid State Ionics* **44**, 21–31 (1990).
16. K. Eguchi, T. Setoguchi, T. Inoue, H. Arai, Electrical properties of ceria-based oxides and their application to solid oxide fuel cells. *Solid State Ionics* **52**, 165–172 (1992).
17. T. Ishihara, H. Matsuda, Y. Takita, Doped $LaGaO_3$ perovskite type oxide as a new oxide ionic conductor. *J. Am. Chem. Soc.* **116**, 3801–3803 (1994).
18. C. Masquelier, Lithium ions on the fast track. *Nat. Mater.* **10**, 649–650 (2011).
19. T. Ohshima, M. Kajita, A. Okuno, Development of sodium-sulfur batteries. *Int. Appl. Ceram. Technol.* **1**, 269–276 (2004).
20. T. Takeuchi, Oxygen sensors. *Sensors Actuators* **14**, 109–124 (1988).
21. N. Imanaka, Y. Kato, A new type of bromide anion conducting solid. *Chem. Commun.*, 1270–1271 (2003).
22. M. R. I. B. Misran, S. Tamura, N. Nunotani, N. Imanaka, Improvement of bromide ion conduction in a lanthanum oxybromide-based solid by adjusting the electronegativity of the cation dopant. *Mater. Lett.* **286**, 129211 (2021).
23. C. Tubandt, E. Lorenz, Molekularzustand und elektrisches Leitvermögen kristallisierter Salze. *Z. Phys. Chem.* **87U**, 513–542 (1914).
24. L. W. Strock, Kristallstruktur des Hochtemperatur-Jodsilbers a-AgJ. *Z. Phys. Chem.* **25B**, 441–459 (1934).
25. A. Smekal, Zum Temperaturgesetz der Ionenleitfahigkeit fester Bleihalogenide. *Z. Phys.* **58**, 322–332 (1929).
26. W. Seith, Die Leifahigkeit fester Bleihalogenide. *Z. Phys.* **56**, 802–808 (1929).
27. C. Tubandt, H. Reinhold, G. Liebold, Bipolare Leitung in festen Elektrolyten. *Z. Anorg. Allg. Chem.* **197**, 225–253 (1931).
28. T. A. Kuku, Ionic transport and galvanic cell discharge characteristics of $CuPbI_3$ thin films. *Thin Solid Films* **325**, 246–250 (1998).
29. A. Kojima, K. Teshima, Y. Shirai, T. Miyasaka, Organometal halide perovskites as visible-light sensitizers for photovoltaic cells. *J. Am. Chem. Soc.* **131**, 6050–6051 (2009).
30. R. A. D. Souza, D. Barboni, Iodide-ion conduction in methylammonium lead iodide perovskite: Some extraordinary aspects. *Chem. Commun.* **55**, 1108–1111 (2019).
31. P. M. Schleitweiler, W. B. Johnson, Conductivity in $PbI_2\text{-}PbO\text{-}B_2O_3$ glasses. *Solid State Ionics* **18-19**, 393–396 (1986).
32. H. Aono, E. Sugimoto, Ionic conductivity of PbI_2-PbO glass. *J. Ceram. Soc. Jpn.* **104**, 235–238 (1996).
33. H. Aono, E. Sugimoto, Y. Sadaoka, Ionic conductivity of $PbX_2\text{-}PbO\text{-}SiO_2$ (X=Cl, Br, I) glasses. *J. Ceram. Soc. Jpn.* **106**, 645–649 (1998).
34. L. G. Sillen, A. L. Nylander, The crystal structure of LaOCl, LaOBr, and LaOI. *Sven. Kem. Tidskr.* **53**, 367–372 (1941).
35. M. Udayakantha, J. V. Handy, R. D. Davidson, J. Kaur, G. Villalpando, L. Zuin, S. Chakraborty, S. Banerjee, Halide replacement with complete preservation of crystal lattice in mixed-anion lanthanide oxyhalides. *Angew. Chem. Int. Ed.* **60**, 15582–15589 (2021).
36. O. Heiniö, M. Leskelä, L. Niinistö, Structural and thermal properties of rare earth triiodide hydrates. *Acta Chem. Scand.* **34A**, 207–211 (1980).
37. A. L. Allred, Electronegativity values from thermochemical data. *J. Inorg. Nucl. Chem.* **17**, 215–221 (1961).
38. N. Imanaka, N. Nunotani, K. Araki, M. Yamane, Exact identification of migrating ion species in scandium tungstate solid electrolyte. *J. Am. Ceram. Soc.* **101**, 1025–1028 (2018).
39. K. Momma, F. Izumi, VESTA: A three-dimensional visualization system for electronic and structural analysis. *J. Appl. Crystallogr.* **41**, 653–658 (2008).
40. H. Iwahara, Proton conducting ceramics and their applications. *Solid State Ionics* **86-88**, 9–15 (1996).
41. C. W. Struck, J. A. Baglio, Estimates for the enthalpy of formation of rare-earth oxyhalides with the P4/*nmm* structure. *Thermochim. Acta* **216**, 45–79 (1993).

Acknowledgments

Funding: This work was supported in part by the JSPS KAKENHI Grant-in-Aid for Scientific Research on Innovative Areas "Mixed anion" (JP19H04698). **Author contributions:** N.I. conceived and supervised this study. M.R.I.B.M. performed the synthesis procedures and experimental investigations. N.I. and N.N. wrote the manuscript. All authors discussed the results and contributed to writing the paper. **Competing interests:** The authors declare that they have no competing interests. **Data and materials availability:** All data needed to evaluate the conclusions in the paper are present in the paper and/or the Supplementary Materials.

Submitted 15 February 2021
Accepted 3 September 2021
Published 22 October 2021
10.1126/sciadv.abh0812

Citation: N. Imanaka, M. R. I. B. Misran, N. Nunotani, Evidence for enormous iodide anion migration in lanthanum oxyiodide–based solid. *Sci. Adv.* **7**, eabh0812 (2021).